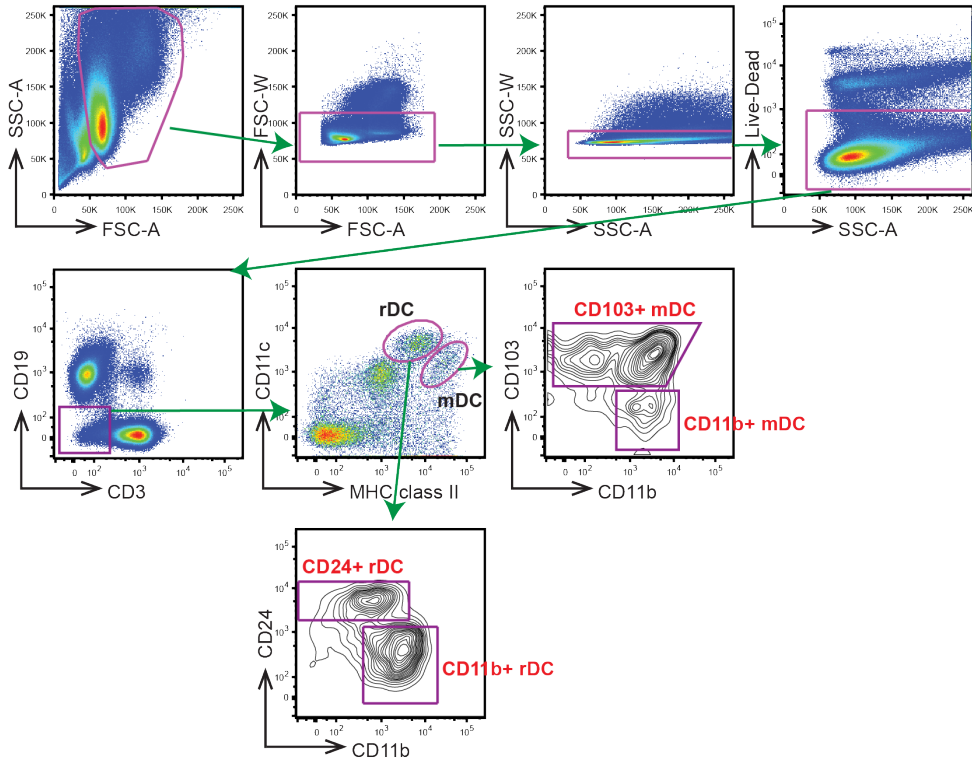


Supplemental Figures

A



B

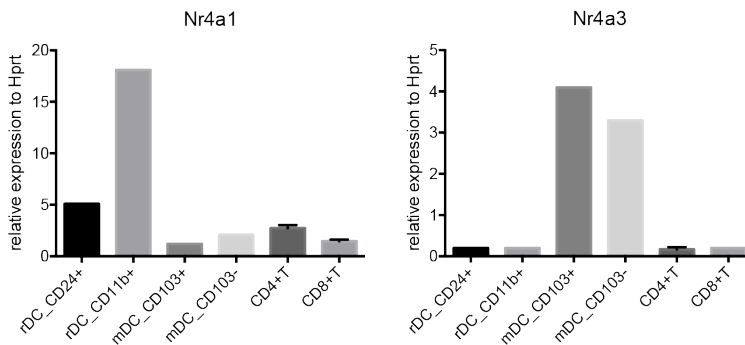


Figure S1.

(A) Gating strategy for lymph node dendritic cell sorting

(B) *Nr4a1* and *Nr4a3* mRNA levels were compared between MLN DC subsets and T cells that were isolated from spleens from *Nr4a3*^{+/+} mice. *Nr4a1* expression was prominent in lymphoid resident DC subsets (rDC) and *Nr4a3* expression was highest in migratory DC subsets (mDC).

Figure S2. MLN DC gating

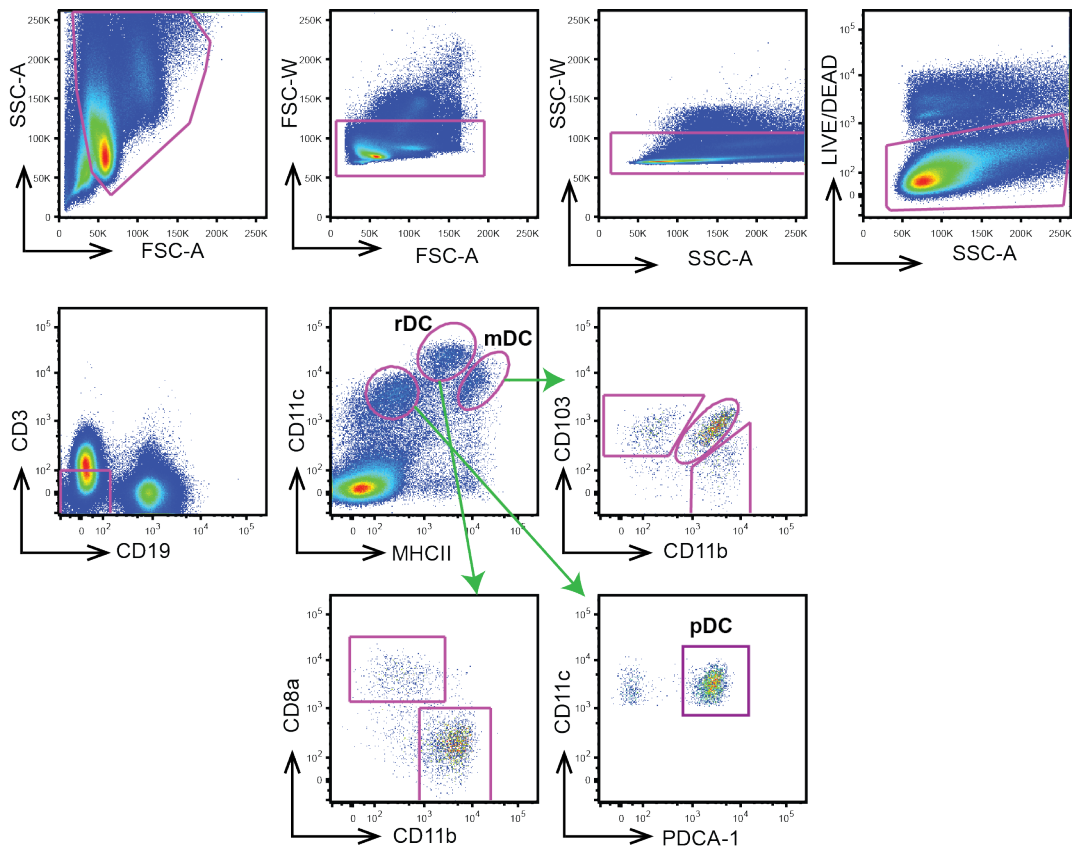


Figure S3. spleen DC gating

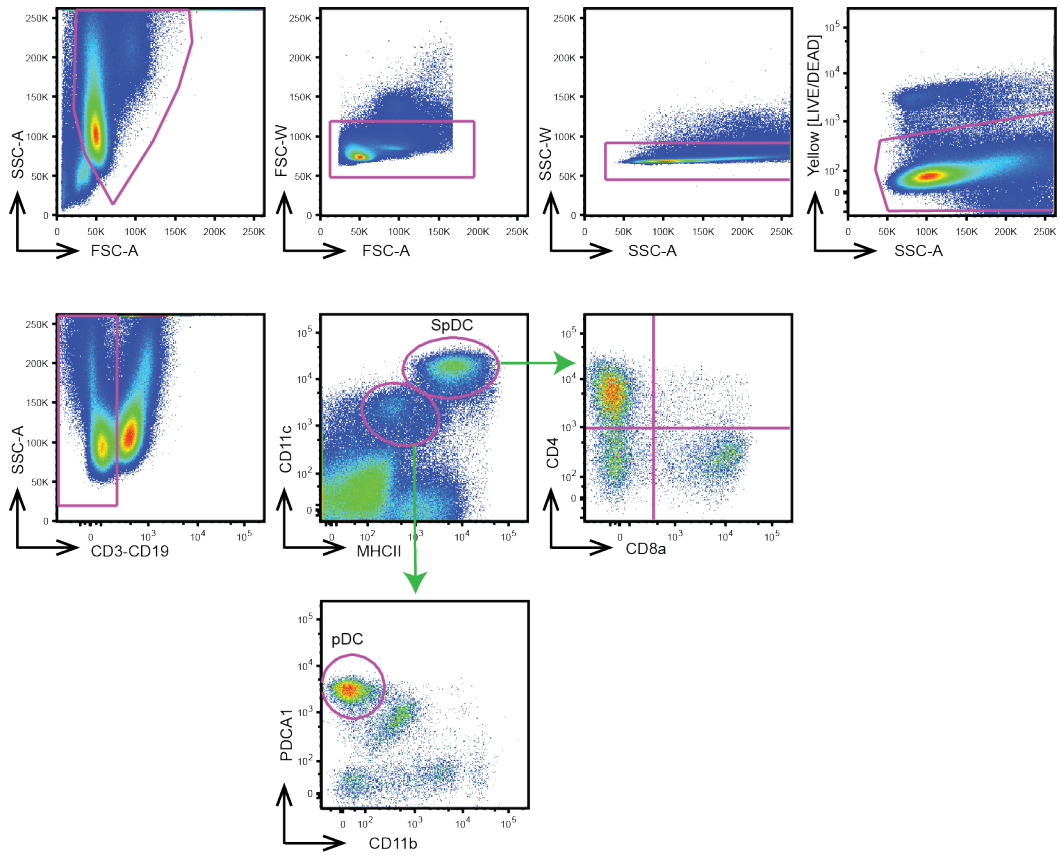
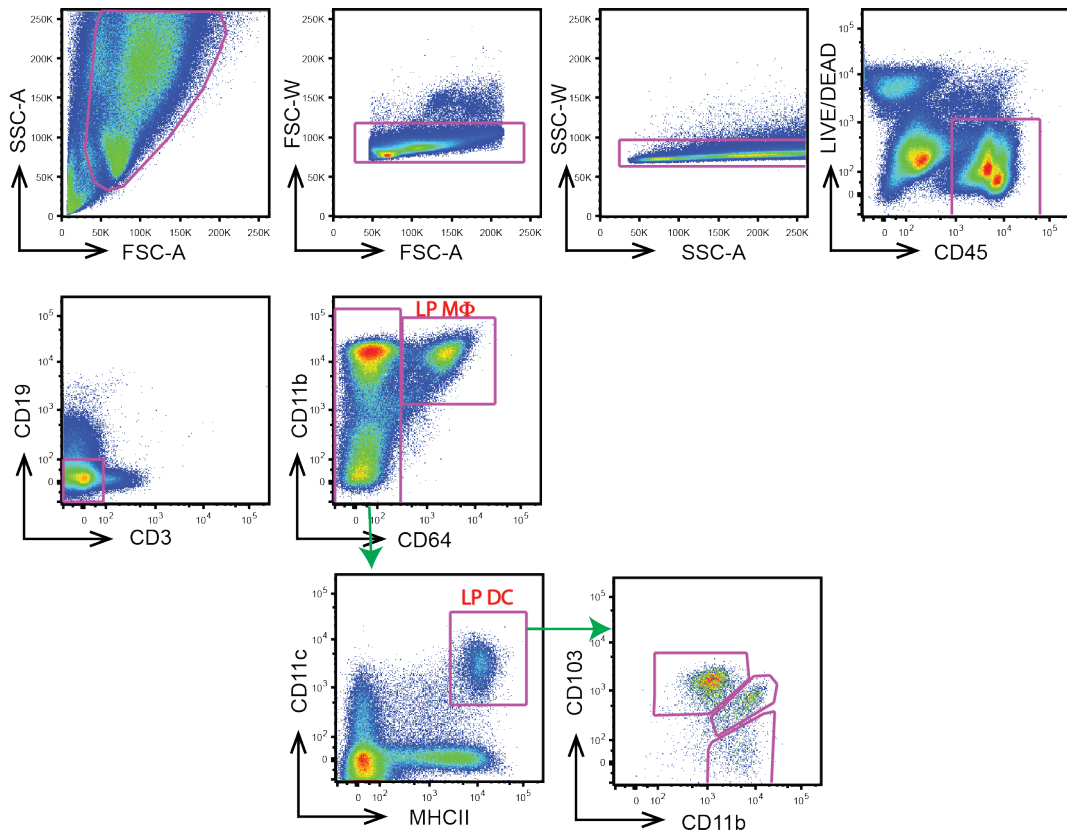


Figure S4. Lamina Propria (LP) DC gating



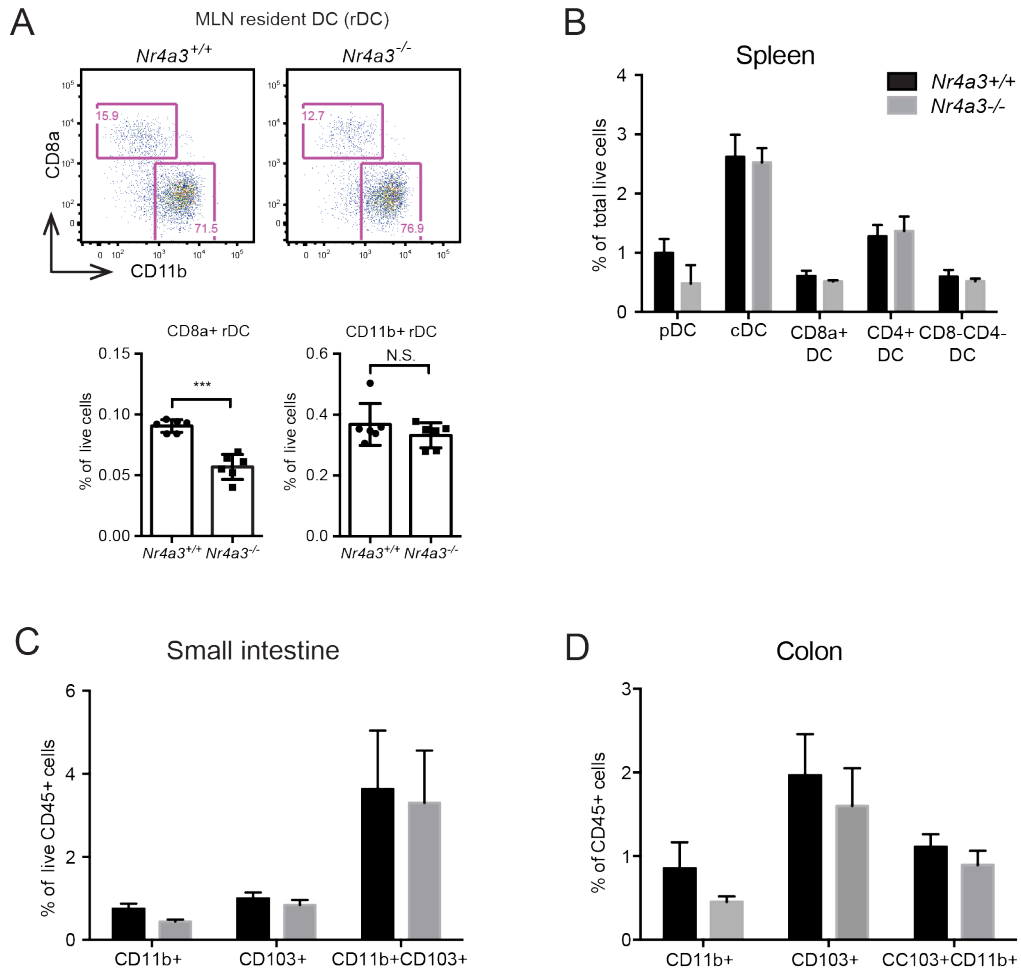


Figure S5. Absence of *Nr4a3* did not much impact on resident DC populations in MLN, small intestine, or colon.

(A) Representative flow cytometry plot and graphical summary of MLN resident DC (rDC) subsets.

(B-D) Graphical summary of flow cytometry analysis of splenic DC (B)

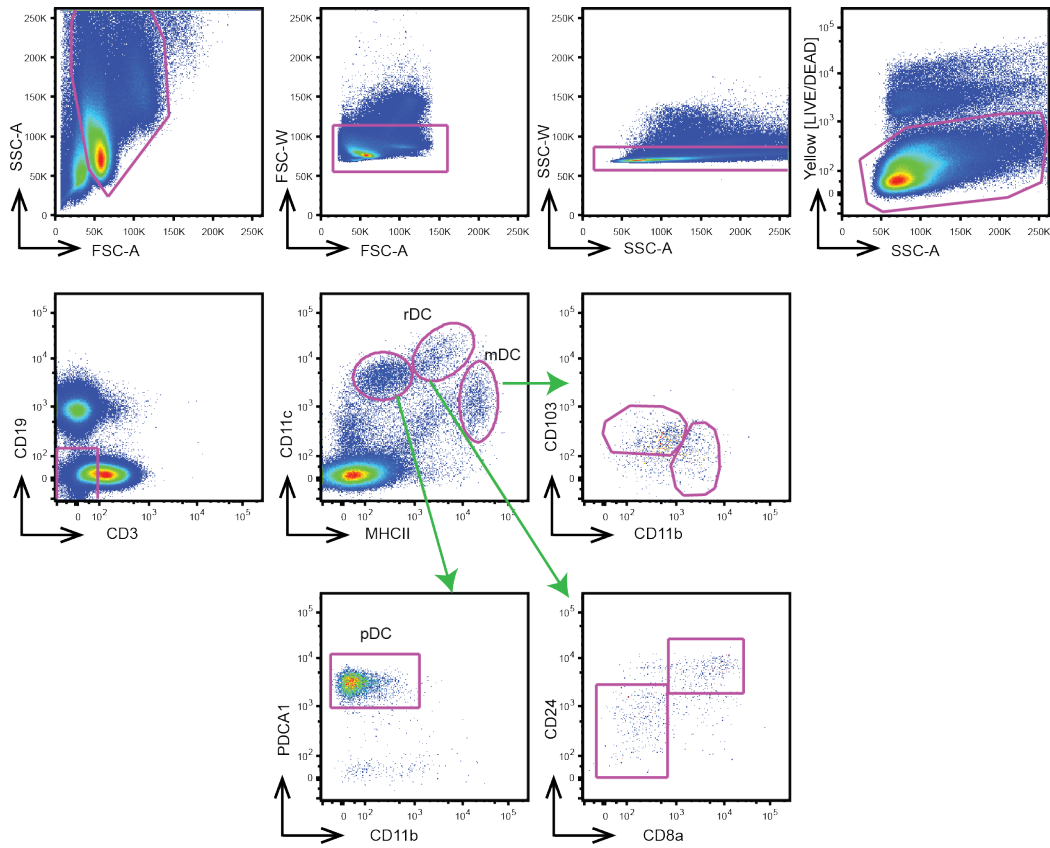
and Lamina Propria DC subsets from WT and *Nr4a3*^{-/-} in small

intestine(C) and colon (D). Black and grey bars indicate *Nr4a3*^{+/+} and

Nr4a3^{-/-} mice, respectively. Results represent two independent

experiments (3 mice per group). *** P < 0.005 by two-tailed Student's T-test.

Figure S6. Skin-draining LN DC gating



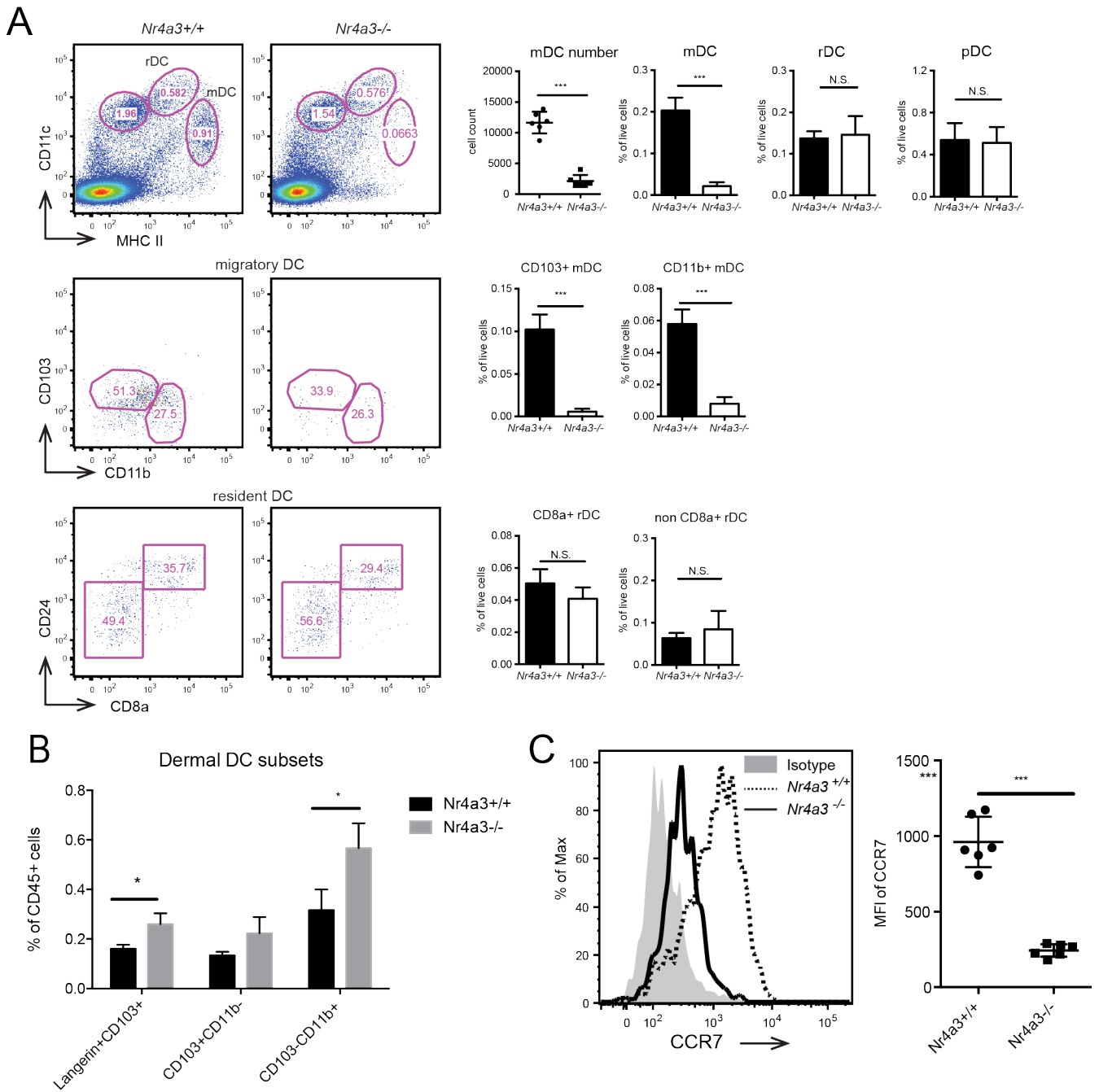


Figure S7. Migratory DCs were significantly lower in skin-draining LN (SLN) from *Nr4a3*^{-/-} mice due to lower CCR7 expression on dermal DC.

SLN DC subsets (A) and dermal DC subsets from ear skin (B) and CCR7 expression on migratory DC from SLN (C) were analyzed from *Nr4a3*^{+/+} and *Nr4a3*^{-/-} mice by flow cytometry. Data are representative of more than four experiments with 3-6 mice per group. Each individual dot represents a single animal. Error bar indicates mean \pm SD. * $P < 0.05$, and *** $P < 0.005$ by two-tailed Student's T-test.

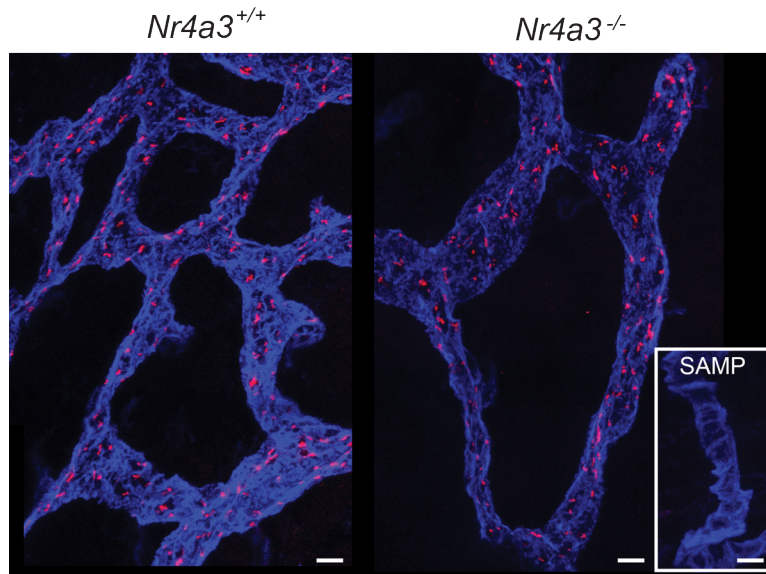


Figure S8. CCL21 expression in ileum was not different between *Nr4a3*^{+/+} and *Nr4a3*^{-/-}.

Terminal ilea from *Nr4a3*^{+/+} and *Nr4a3*^{-/-} mice were collected and fixed with 4% paraformaldehyde in PBS for 18hrs. After washing with PBS, tissues were permeabilized in PBS with 2% saponin, 2% FBS, and 0.05% of Sodium Azide.

Tissues were stained with eFlour 660-conjugated monoclonal rat-anti-mouse Lyve-1 antibodies (1:100, ALY7, eBioscience) and with a polyclonal goat-anti-mouse CCL21 antibodies (1:100, AF457, R&D) directly labeled with a CF543 mix-n-stain antibody labeling kit (Biotium) for 18hrs in a 100 μ l volume. After washing, samples were mounted in Prolong Gold Antifade reagent (Life Technologies) with a #1.5 borosilicate glass cover slip. An SP5 resonant laser-scanning confocal system mounted on a DM 6000 upright microscope (Leica Microsystems) with a 25X water-immersion objective (numerical aperture 0.95) was used for fluorescence microscopy. Image acquisition was done at room temperature using Leica Application Suite Advanced Fluorescence software. Images used for three-dimensional reconstructions were acquired with 2 μ m Z step size. CCL21 labeling (pink) was visualized with 543-nm excitation, 488-nm and 633-nm excitation wavelengths were used to visualize eFluor660-labelled lymphatic vessels (blue). Fluorescent signals were detected with internal photomultiplier tubes. Maximum intensity projection images of CCL21 and lymphatic vessels were created in Fiji (Schindelin J et al. Fiji: an open-source platform for biological-image analysis. Nat. Methods 2012;9(7):676–82).

Insert: Intestine from SAMP1/YitFc mouse, which have greatly reduced level of Ccl21 expression (Mikulski Z et al. SAMP1/YitFc mice develop ileitis via loss of CCL21 and defects in dendritic cell migration. Gastroenterology 2015;148(4):783–793.e5.) was used as a control for Ccl21 antibody specificity. Bar = 20 μ m. Shown are representative images of tissue collected from 3 mice per group. The experiment was repeated two times.

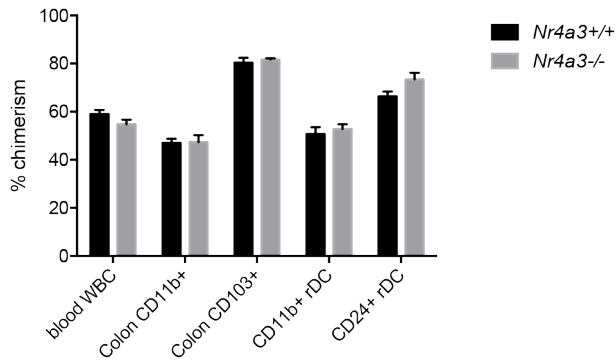


Figure S9. Reconstitution of Colon and MLN resident DC subsets were not affected by the absence of *Nr4a3*.

Mixed bone marrow chimera experiment was performed as described in Methods. Donor DC populations from colon and MLN were analyzed by flow cytometry. Percentage of CD45.2(*Nr4a3*^{+/+} or *Nr4a3*^{-/-}) was calculated from total donors that include CD45.2 and CD45.1. Bone marrow reconstitution was assessed from blood. Result is a representative of two independent experiments (3-4 mice per group).

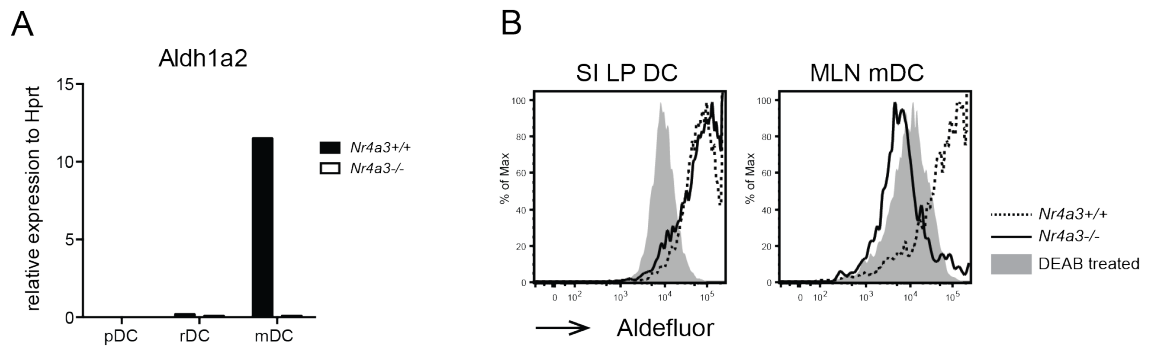


Figure S10. Migratory DCs from *Nr4a3*^{-/-} MLN did not express Retinaldehyde dehydrogenase 2 (*Raldh2*, *Aldh1a2*).

(A) *Aldh1a2* mRNA was measured from FACS-sorted MLN DC subsets by Q-RT PCR. (B) RALDH enzyme activity from LPDC and MLN DC was measured by Aldefluor assay (Stem Cell Technologies). Dotted line and black line indicate *Nr4a3*^{+/+} and *Nr4a3*^{-/-}, respectively. Grey shade represents *Nr4a3*^{+/+} cells treated with RALDH inhibitor DEAB as a negative control. Data represent 2 independent experiments (3 mice per group).

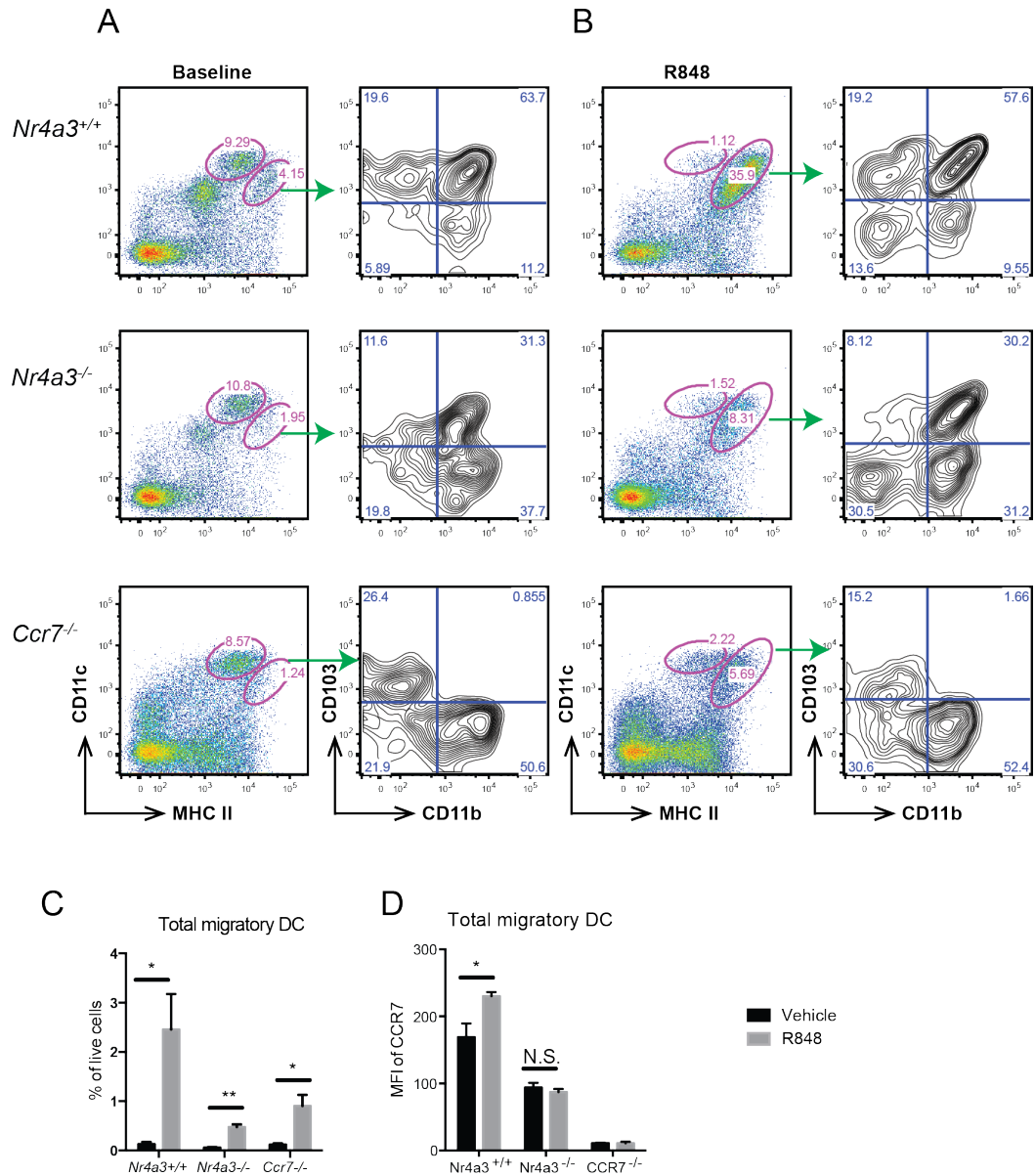
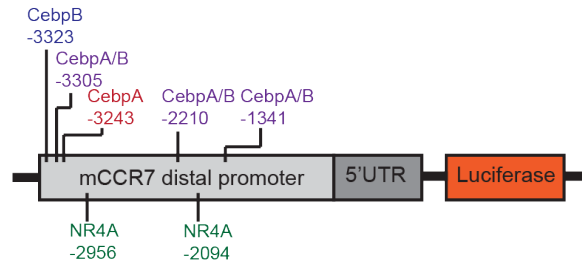


Figure S11. R848 treatment did not rescue CD103⁺ DC migration to MLN. 8-12 week old *Nr4a3*^{+/+}, *Nr4a3*^{-/-}, and *Ccr7*^{-/-} mice (3 mice per group) were given vehicle (0.8%DMSO in water, A) or 10 μ g of R848 (B) per mouse by oral gavage. After 14hrs, MLNs were collected and MLN DCs were analyzed by flow cytometry. Changes of total migratory DC and MFI of CCR7 were plotted (C). Error bar indicated mean \pm SD. P-value was calculated by two-tailed Student's T-test. ‘*’, ‘**’, and ‘***’, represent P < 0.05, P < 0.01, P < 0.005, respectively.

A



B

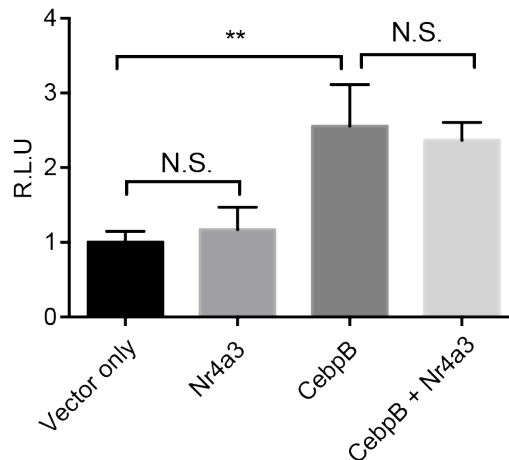


Figure S13. NR4A3 does not activate *Ccr7* promoter by direct binding.

(A) 5 C/EBP α and β binding motifs and 2 NR4A binding motifs were predicted in 3.3kb sequence upstream of the transcriptional start site of the murine *Ccr7* promoter using MacVector software as described in Methods.

(B) This 3.3kb *Ccr7* sequence was cloned into pGL4 luciferase vector (Promega). *Nr4a3* and C/EBP beta cDNA expression clones were cloned into pCMV6-Entry vector (OriGene, Rockville, MD). Constitutive beta-galactosidase plasmid and the *Ccr7* pGL4 plasmids were co-transfected with cDNA expressing plasmids into RAW264.7 or 293T cell lines. After 18 hrs, cells were lysed and a dual luciferase reporter assay was performed by using a single automatic injection Mithras (Berthold technologies) luminometer following the manufacturer's protocol (Promega). Transfections were performed in triplicate. Ratios of Luciferase activity and beta-galactosidase activity were normalized by empty reporter construct values. (B) Results represent 3 experiments. **P < 0.001, by Student's T-test.

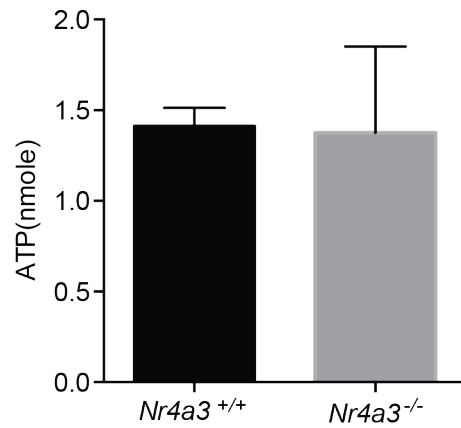


Figure S14. ATP content of *Nr4a3*^{-/-} DC was not different from *Nr4a3*^{+/+} DC. CD11c⁺ cells were isolated by CD11c micro beads (Miltenyi Biotech) from Da8 BM culture. Intracellular ATP concentration was measured from 500,000 cells of CD11c⁺BMDC by CellTiter-Glo® Assay kit (Promega). Result represents two independent experiments.